5754 J. Phys. Chem. A **1998,** *102,* 5754−5762

Two Channels of Electron Transfer Observed for the Reaction of *n*-Butyl Chloride Parent Radical Cations with Naphthols and Hydroxybiphenyls

H. Mohan,[†] R. Hermann,[‡] S. Naumov,[§] J. P. Mittal,[†] and O. Brede*,[‡]

Chemistry Division, Bhabha Atomic Research Centre, Trombay, Mumbai 400 085, India, University of Leipzig, Interdisciplinary Group Time-Resolved Spectroscopy, Permoserstrasse 15, D-04303 Leipzig, Germany, and Institute of Surface Modification, Permoserstrasse 15, D-04303 Leipzig, Germany

Received: January 22, 1998; In Final Form: March 30, 1998

Pulse radiolysis of naphthols (NpOH) and hydroxybiphenyls (ByOH) in *n*-butyl chloride (BuCl) at room temperature exhibits electron transfer at a bimolecular rate constant of (1.0−2.8) × 10^{10} dm^3 mol^{-1} s^{-1}. The experiments reveal the direct formation of two types of transients: phenol type radical cations ($NpOH^{•+}$, $ByOH^{•+}$) and phenoxyl type radicals ($NpO^{•}$, $ByO^{•}$). This is explained by a mechanism involving two different electron-transfer channels. The solute radical cations exhibit two optical absorption bands in the 570−650 and 360−460 nm regions and undergo electron transfer with triethylamine and proton transfer with ethanol with bimolecular rate constants of (4−12) × 10^9 and (3−6) × 10^8 dm^3 mol^{-1} s^{-1}, respectively. $NpO^{•}$ and $ByO^{•}$ have relatively long lifetimes and show absorption bands in the 340−400 and 470−540 nm regions. By way of comparison, these phenoxyl type radicals are separately generated by pulse radiolysis in aqueous alkaline solution containing sodium azide, i.e., by oxidation of the solutes with $N_3^{•}$ radicals. Under these conditions, the phenoxyl radicals decay by second-order kinetics with $2k = (1.2-4.5) \times 10^8$ dm^3 mol^{-1} s^{-1}. The various modes of formation and decay of the phenolic radical cations are analyzed over a wide range of dose rate and solute concentrations. In comparison to radical cations of one-ring phenols, the increased stability of $NpOH^{•+}$ and $ByOH^{•+}$ is explained by the delocalization of the positive charge over the whole aromatic system, a postulate supported by open-shell quantum chemical calulations.

1. Introduction

Increasing attention has been devoted to electron-transfer processes involving phenols and their substituted derivatives, since they play an important role in the stabilization of polymers, food, and oils, etc.[1,2] Their antioxidative properties are understood in terms of electron and H atom donor ability.[3] Owing to their low ionization potential and the weak O−H bond, phenols and substituted derivatives act as model systems for understanding the antioxidative mechanism.[4,5] Because of their low pK_a value and their instability even under nonprotic conditions, phenol radical cations can hardly be detected and phenoxyl radicals are usually the first observable oxidation products of one-electron-transfer oxidation.[6] Hence, in polar solutions phenol radical cations have been observed in strongly acidic media and characterized by EPR.[7,8] In nonpolar solvents, the radical cations of phenols and substituted derivatives were characterized by optical absorption and EPR spectra taken in glasses at 77 K[1,9,10] as well as by pulse radiolysis at room temperature in nonpolar solutions.[1]

Pulse radiolysis of phenols (ArOH) in *n*-butyl chloride (BuCl) provided evidence of the formation of solute radical cations ($ArOH^{•+}$) with very broad and unspecific optical absorption bands.[1] The time profiles gave a clear indication of the kinetics of the formation and decay of $ArOH^{•+}$. Hence, the bimolecular rate constants for electron transfer from solute to solvent radical cations were determined to be in the range (1−2) × 10^{10} dm^3 mol^{-1} s^{-1}. It was found that the solvent radical cations react with phenols (ArOH) by electron transfer (reaction 1a) as well as deprotonation (reaction 1b), the latter process yielding solvent-stabilized protons:

$$BuCl^{•+} \rightarrow ArOH^{•+} + BuCl \tag{1a}$$

$$\rightarrow ArO^{•} + H^{+}\,(BuCl) \tag{1b}$$

Since at room temperature in liquid phase the rapidly formed phenoxyl radicals dominate, reaction 1b describes the main channel of the reaction of parent radical cations with the phenolic solute. Owing to delocalization of the positive charge, in the case of *p*-methoxy-substituted phenols, the increase in kinetic and thermodynamic stability resulted in the domination of reaction channel 1a. Furthermore, the decay of $ArOH^{•+}$ of normal phenols proceeds by neutralization (reaction 2) as well as deprotonation (reaction 3), the latter process mainly being unimolecular:[1]

$$ArOH^{•+} + Cl^{-} \rightarrow \text{neutral products} \tag{2}$$

$$\rightarrow ArO^{•} + H^{+} \tag{3}$$

To understand the mechanism of electron-transfer processes of phenols and the effect of solute structure on various reaction channels, pulse radiolysis studies of naphthols and hydroxybiphenyls in butyl chloride were initiated. The extended aromatic moiety is expected to play an important role in the

---

[†] Bhabha Atomic Research Centre.

[‡] University of Leipzig.

[§] Institute of Surface Modification.

S1089-5639(98)00843-3 CCC: $15.00

stabilization of the solute radical cations as well as in the conceivable formation of dimers of charge-transfer character, analogous to other aromatic radical cations (ref 11a). In this paper we report on pulse radiolysis of naphthols and hydroxybiphenyls under the aspect of radical cation kinetics.

2. Experimental Section

2.1. Pulse Radiolysis. The liquid samples were irradiated with high-energy electron pulses (1 MeV, 16 ns pulse duration) generated by a pulse transformer type accelerator ELIT (Institute of Nuclear Physics, Novosibirsk, Russia). The dose delivered per pulse was measured with an electron dosimeter and was usually around 50 Gy per pulse. The detection of the transient species was carried out by the optical absorption technique, which consists of a pulsed xenon lamp (XBO 900, Osram), a Spectra Pro-500 monochromator (Acton Research Corporation), an IP28 photomultiplier (Hamamatsu Photonics), and a 1 GHz digitizing oscilloscope (TDS 640, Tektronix). Further details are given elsewhere.[1]

Pulse radiolysis experiments were performed in N_2-saturated *n*-butyl chloride solutions. Reaction with $N_3^•$ radicals, generated via reactions 3a and 3b, was carried out in N_2O-saturated aqueous solution of N_3^- (2×10^{-2} mol dm^{-3}, pH = 10). The solutions continuously flowed through the sample cell with a path length of 1 cm.×

2.2. Laser Photolysis. Laser photolysis experiments were carried out using the fourth harmonic (266 nm) from a Quanta Ray GCR-11 Nd:YAG laser (Spectra-Physics Lasers). The pulse duration (fwhm) was measured to be 3 ns, and the pulse energy was ~10 mJ. The N_2-saturated solution continuously flowed through a quartz cell (0.3 cm × 0.3 cm). The probe light of a pulsed 400 W xenon lamp (XBO-400, Osram) passed through a SpectraPro-275 monochromator (Acton Research Corporation) to a R955 photomultiplier tube (Hamamatsu Photonics). The output signals were recorded on a 500 MHz digitizing oscilloscope (DSA 602 A, Tektronix). Other details are given elsewhere.[1]

2.3. Chemicals. Naphthols (1- and 2-NpOH) and hydroxybiphenyls (2-, 3-, and 4-ByOH) were commercially available. *n*-Butyl chloride (BuCl, Merck) was additionally purified by passing it through a column of an activated molecular sieve (×13). The studies in aqueous solutions were performed in purified water (Millipore, Milli-Q plus system).

3. Results and Discussion

The electrons produced during the radiolysis of BuCl are immediately scavenged by the solvent molecules by a dissociative electron capture process to form Cl^- anions. The highly mobile positively charged holes ($h^{•+}$) move through the solvent and are localized as $BuCl^{•+}$ or butene radical cations ($Bu^{•+}$).[11b]

$$BuCl \rightarrow h^{•+}, e_{solv}^{-} \tag{4}$$

$$h^{•+} + BuCl \rightarrow BuCl^{•+} \tag{5a}$$

$$\rightarrow Bu^{•+} + HCl \tag{5b}$$

$$e_{solv}^{-} + BuCl \rightarrow Bu^{•} + Cl^{-} \tag{6}$$

In the absence of any added solute, the transient optical absorption spectrum during pulse radiolysis of N_2-saturated BuCl exhibits broad absorption peaking near 500 nm caused by $BuCl^{•+}$ (see Figure 1). These positively charged species decay by fragmentation (reaction 5b) and the charge neutralization process (reaction 7).

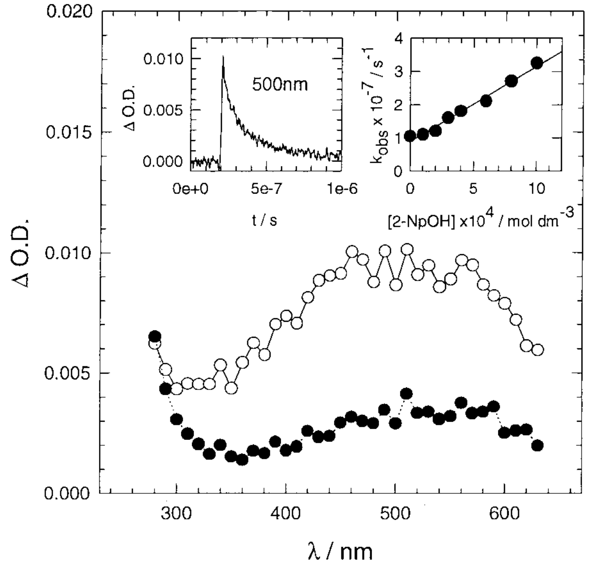

Figure 1. Transient optical absorption spectra taken in the pulse radiolysis of pure *n*-butyl chloride purged with N_2: (○) immediately after the pulse; (●) after 100 ns. The insets show a typical time profile and the Stern−Volmer plot to determine the rate of electron transfer from 2-NpOH to the solvent radical cation.

$$BuCl^{•+}, Bu^{•+} + Cl^{-} \rightarrow \text{products} \tag{7}$$

BuCl was employed as a solvent for the generation and investigation of solute radical cations due to (i) its high ionization potential (I_{gas} = 10.7 eV), (ii) formation of very short-lived (τ = 90 ns) transient species ($BuCl^{•+}$) with a broad and very small absorption in the 300−500 nm region, and (iii) the relatively high yield of free ions (G = 0.3). Figure 1 demonstrates this situation using optical absorption spectra and a time profile taken in pure *n*-butyl chloride purged with nitrogen.

3.1. Pulse Radiolysis of Naphthols. *Pulse Radiolysis of 2-NpOH.* In the presence of 2-NpOH (I_{gas} = 7.8 eV), the positively charged species generated from the radiolysis of BuCl react by an electron-transfer process (reaction 8), whereas radical species ($Bu^•$) may react by H atom abstraction (reaction 9).

$$BuCl^{•+} + 2\text{-NpOH} \rightarrow 2\text{-NpOH}^{•+} + BuCl \tag{8}$$

$$Bu^{•} + 2\text{-NpOH} \rightarrow 2\text{-NpO}^{•} + Bu \tag{9}$$

The rate constants of these reactions, however, differ by some orders in magnitude. Upon addition of the naphthols, the transient absorption of $BuCl^{•+}$ at 500 nm (cf. time profile given in the inset of Figure 1) showed accelerated decay and the pseudo-first-order rate constant (k_{obs}) increased linearly with solute concentration (1−10) × 10^{-4} mol dm^{-3}. The bimolecular rate constant calculated from the Stern−Volmer plot (inset of Figure 1) of reaction 8 was found to be $k_8 = 2 \times 10^{10}$ dm^3 mol^{-1} s^{-1} (Table 1). The intercept of the Stern−Volmer plot (Figure 1) represents the decay of $BuCl^{•+}$ in the absence of any added solute and corresponds to a lifetime of 90 ns.

The transient optical absorption spectrum obtained during pulse radiolysis of an N_2-saturated solution of 2-NpOH (5×10^{-3} mol dm^{-3}) in BuCl 300 ns after the pulse, showed an

TABLE 1: Bimolecular Rate Constants for Electron Transfer from Solutes to Solvent Radical Cation ($BuCl^{\bullet +}$) (Reaction 1a)

solute	1-NpOH	2-NpOH	2-ByOH	3-ByOH	4-ByOH
electron transfer rate constant × 10^{-10} ($dm^3mol^{-1}s^{-1}$)	1.0	2.0	2.8	1.9	1.8

TABLE 2: Spectral Parameters for the Transient Species Formed during Pulse Radiolysis of N_2-Saturated BuCl Containing Different Solutes (ArOH)

Ar	$\lambda(ArOH^{\bullet +})$ (nm)	$\lambda(ArO^{\bullet})$ (nm)	$\lambda(ArOH)_2^{\bullet +}$ (nm)
1-NpOH	380	340	420
	420	390	
	580	530	
2-NpOH	360	350	410
	460	380	
	570	475	
2-ByOH	360	360	440
	380	400	
	600		
3-ByOH	390	340	420
	650	530	
4-ByOH	390	340	430
	650	540	

absorption band at 350 nm with a shoulder at 380 nm, broad absorption between 430 and 490 nm with a sharp peak at 475 nm, and broad absorption in the 530−650 nm region (Figure 2a). During this time (0.3 μs after the pulse), the solvent transient species ought to be decayed and the transient spectrum observed is clearly due to the transient species generated from 2-NpOH. Analysis of absorption time profiles (Figure 2b) revealed that the band at 570 nm is relatively short-lived and decays by first-order kinetics at $k = 6.6 \times 10^5\ s^{-1}$. Absorption at other wavelengths chosen was relatively long-lived and displayed mixed kinetics. This suggests the presence of more than one species, tentatively interpreted as a solute cation and a solute radical.

Identification of Transient Species. To determine the nature of these phenolic species, additional scavengers were used. In the presence of low concentration (1 mM) of triethylamine (TEA), a positive charge scavenger, the absorption band at 570 nm was completely quenched (Figure 2a) and a considerable decrease in absorption was observed at 360 nm. Absorption at other wavelengths only showed a small decrease (Figure 2a). Analogous to earlier studies of phenols,[1] the short-lived transient absorption, which was quenched by positive charge scavengers, was attributed to the solute radical cation ($2\text{-}NpOH^{\bullet +}$). The relatively long-lived absorption (Figure 2a) showed very little inpact on TEA and was classified as that of the naphthoxyl radicals ($2\text{-}NpO^{\bullet}$). The difference between the spectra (in the presence and absence of TEA) gives the absorption spectrum of $2\text{-}NpOH^{\bullet +}$ exhibiting bands at 360 and 570 nm. This enabled the positions of the transient absorption bands of $2\text{-}NpOH^{\bullet +}$ and $2\text{-}NpO^{\bullet}$ to be determined. The corresponding data are given in Table 2.

To verify the spectrum of naphthoxyl radicals ($2\text{-}NpO^{\bullet}$), pulse radiolysis studies were performed in aqueous solutions. The optical absorption spectrum of an aqueous solution of 2-NpOH revealed that it exists in deprotonated form at pH ≥ 10 ($pK_a = 8.5$). Therefore, one-electron oxidation of $2\text{-}NpO^-$ by $N_3^{\bullet}$ radicals, a specific one-electron oxidant,[12] ought to form $2\text{-}NpO^{\bullet}$ radicals via reaction 10c. The azide radical was generated via reactions 10a and 10b.

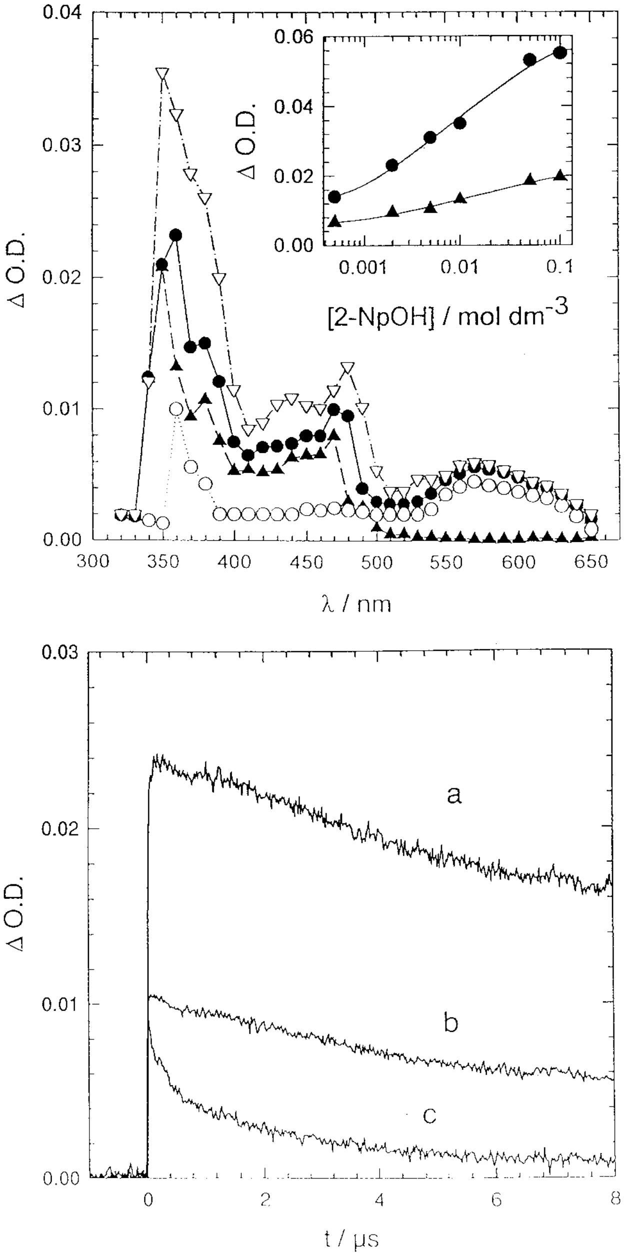

Figure 2. (a) Transient optical absorption spectra obtained in the pulse radiolysis of N_2-saturated solution of 2-NpOH (5×10^{-3} mol dm^{-3}) in BuCl in the absence (●) and in the presence of 1×10^{-3} mol dm^{-3} TEA (▲). The difference of absorption spectra is shown as ○. The transient spectrum of 2-NpOH (1×10^{-2} mol dm^{-3}) in BuCl is given by ▽. The inset shows the variation of absorbance as a function of solute concentration (scavenger curve) at 350 nm (●) and 475 nm (▲). (b) Absorption time profiles on pulse radiolysis of N_2-saturated solution of 2-NpOH (5×10^{-3} mol dm^{-3}) in BuCl at 360 (a), 470 (b), and 570 (c) nm.

$$N_2O + e_{aq}^{-} \rightarrow {}^{\bullet}OH + OH^{-} + N_2 \qquad (10a)$$

$${}^{\bullet}OH + N_3^{-} \rightarrow N_3^{\bullet} + OH^{-} \qquad (10b)$$

$$2\text{-}NpO^{-} + N_3^{\bullet} \rightarrow 2\text{-}NpO^{\bullet} + N_3^{-} \qquad (10c)$$

Figure 3 shows the transient optical absorption spectrum obtained during pulse radiolysis of an N_2O-saturated aqueous solution of NaN_3 (3×10^{-2} mol dm^{-3}, pH = 10) containing

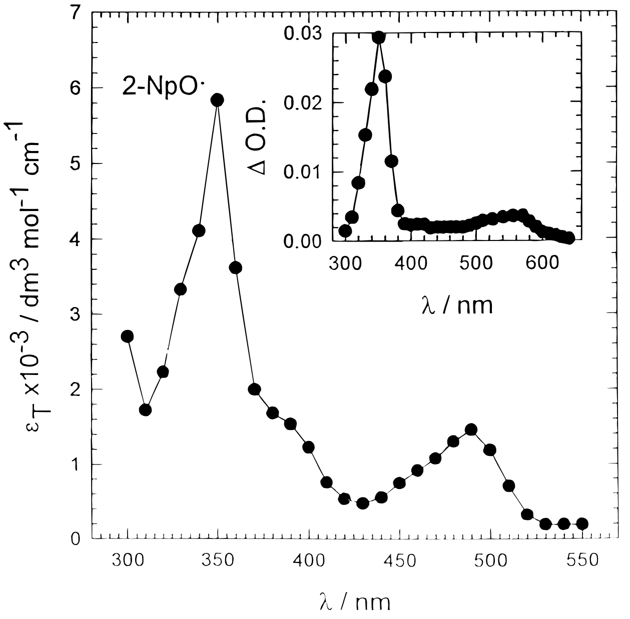

Figure 3. Transient optical absorption spectrum obtained during pulse radiolysis of an N_2-saturated aqueous solution of NaN_3 (3×10^{-2} mol dm^{-3}, pH = 10) and 2-NpOH (2×10^{-4} mol dm^{-3}). The inset shows the absorption spectrum taken immediately after the pulse with 3-ByOH (2×10^{-4} mol dm^{-3}) under the same conditions.

TABLE 3: Kinetic and Spectral Parameters for ArO$^\bullet$ Radicals Formed during the Reaction of $N_3^\bullet$ with ArO$^-$ (Reaction 10)

Ar	λ_{max} (nm)	$k \times 10^{-9}$ (dm^3 mol^{-1} s^{-1})	$\epsilon_{max} \times 10^{-3}$ (dm^3 mol^{-1} cm^{-1})	decay ($2k$) × 10^{-8} (dm^3 mol^{-1} s^{-1})
1-NpOH	330	6.6	9.82	4.4
	400		1.76	
	530		0.72	
2-NpOH	350	6.2	5.84	4.5
	390		1.50	
	490		1.46	
2-ByOH	350	1.7	2.96	3.4
	400		1.07	
3-ByOH	350	0.6	0.93	1.2
	540		0.17	
4-ByOH	350	4.6	1.78	2.1
	540		0.43	

2-NpOH (2×10^{-4} mol dm^{-3}), which exhibits absorption bands with λ_{max} at 350 and 480 nm and a shoulder in the 370−390 nm region (Table 3). The spectrum qualitatively matched that obtained in BuCl (Figure 2a). The bimolecular rate constant (k_{10c}) was determined to be $k_{10c} = (6.2 \pm 0.3) \times 10^9$ dm^3 mol^{-1} s^{-1}. The entire spectrum is due to 2-NpO$^\bullet$, which decays by second-order kinetics with $2k = 4.5 \times 10^8$ dm^3 mol^{-1} s^{-1} (Table 3).

The radical cations of phenols (ArOH) were photolytically ($\lambda = 266$ nm) generated by a two-photon absorption process (reaction 11) in *n*-butyl chloride solution in which the electron is immediately converted into Cl$^-$ (cf. reaction 6).[1]

$$\mathrm{ArOH} + 2h\nu \rightarrow \mathrm{ArOH}^{\bullet +} + \mathrm{e_{solv}}^{-} \qquad (11)$$

However, in the laser photolysis of NpOH, we failed to observe 2-NpOH$^{\bullet+}$. Instead, we obtained the triplet−triplet absorption spectrum of 2-NpOH^{T1} peaking at 430 nm.[13a] Obviously, the singlet−triplet intersystem crossing efficiency was too high and optical conditions for both singlet and triplet ionization were unfavorable under our experimental conditions.

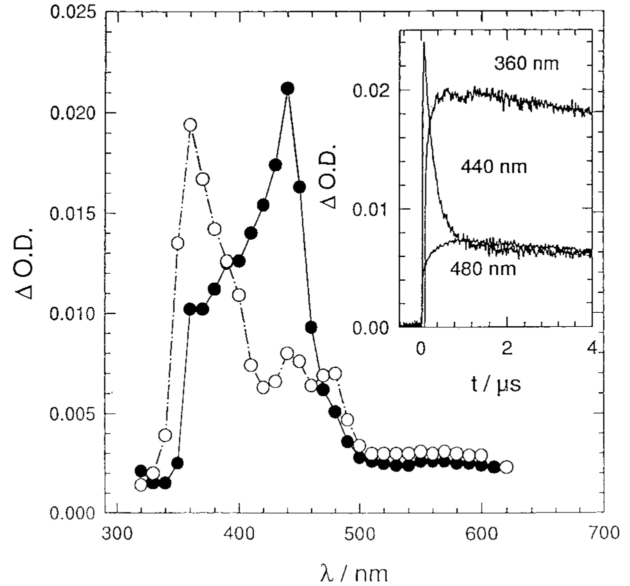

Figure 4. Transient optical absorption spectra obtained in pulse radiolysis of an N_2-saturated solution of 1-NpOH (1×10^{-2} mol dm^{-3}) and chloranil (6×10^{-4} mol dm^{-3}) in benzene 0.1 μs (●) and 0.8 μs (○) after the pulse. The inset shows time profiles at representative spectral points.

Triplet-Sensitized Electron Transfer. In view of the high efficiency of triplet formation, the solute radical cations could be generated by a triplet-sensitized electron-transfer process. Chloranil (CA = 2,3,5,6-tetrachloro-1,4-benzoquinone) has a greater electron affinity than 2-NpOH^{T1} and, therefore, should be able to form anion radicals in accordance to reaction 12b.

$$\mathrm{C_6H_6T1} + \text{2-NpOH} \rightarrow \text{2-NpOH}^{T1} + \mathrm{C_6H_6} \qquad (12a)$$

$$\text{2-NpOH}^{T1} + \mathrm{CA} \rightarrow [\mathrm{NpOH}^{T1}\cdots\mathrm{CA}] \rightarrow [\mathrm{NpOH}^{\bullet+}\cdots\mathrm{CA}^{\bullet-}] \rightarrow \text{2-NpO}^{\bullet} + \mathrm{HCA}^{\bullet} \qquad (12b)$$

This was performed using pulse radiolysis of benzene solutions in which the naphthol triplets are formed by scavenging the solvent triplets caused by reaction 12a. Figure 4 shows the transient optical absorption spectra obtained during pulse radiolysis of an N_2-saturated solution of 2-NpOH (1×10^{-2} mol dm^{-3}) in benzene containing a low concentration of chloranil (6×10^{-4} mol dm^{-3}). Under these conditions, the primarily formed benzene triplet[13b] rapidly transfers its energy to 2-NpOH, and the transient optical absorption spectrum taken 0.1 μs after the pulse represents the triplet−triplet absorption spectrum of 2-NpOH^{T1}. During the course of reaction 12b the transient optical absorption spectra 0.8 μs after the pulse showed absorption bands peaking at 360, 440, and 480 nm and a long tail to the red range. Regarding the spectra of 2-NpOH$^{\bullet+}$ (Figure 2a) and of 2-NpO$^\bullet$ (Figure 3), the bands at 360 and 480 nm correspond well to those of the naphthoxyl radical (Table 2). Because of the similiarity of the blue band of the radical cation and the radical, at first glance the 10 nm shift of the radical band in benzene compared with that in water seems to suggest the formation of 2-NpOH$^{\bullet+}$. However, the 480 nm band itself and the relation between it and the blue band clearly argue for the 2-NpO$^\bullet$. Following lengthy consideration of the absorption behavior of the chloranil semiquinone radical by Gschwind and Haselbach,[13c] the 440 nm peak and the flat absorption between 500 and 600 nm ought to be caused by this radical species CA$^\bullet$. Judging by the fast rate of process 12, we can conclude that the triplet-sensitized electron transfer indeed took place but was

TABLE 4: Bimolecular Rate Constant for the Reaction of Further Additives with Solute Radical Cations: TEA (Electron Transfer 13a), EtOH (Deprotonation 13b)

solutes	additives	rate constant $\times 10^{-9}$ ($\mathrm{dm^3\,mol^{-1}\,s^{-1}}$)
1-NpOH	TEA	7.0
	EtOH	0.5
2-NpOH	TEA	4.0
	EtOH	0.6
2-ByOH	TEA	11.6
	EtOH	0.3
3-ByOH	TEA	9.6
	EtOH	
4-ByOH	TEA	12.0
	EtOH	

followed by subsequent rapid proton transfer within the intermediate contact ion pair, finally resulting in radicals instead of the expected ions.

Electron-Transfer Reactions Involving Naphthol Radical Cations. To determine the kinetics of electron-transfer processes, the decay of the 570 nm band of 2-NpOH$^{\bullet+}$ was analyzed for increasing concentrations of TEA, which accelerated its decay. The pseudo-first-order rate constant (k_{obs}) was found to be proportional to the TEA concentration $(1-4) \times 10^{-4}$ mol dm^{-3} from which k_{13a} was calculated to be 4×10^9 dm^3 mol^{-1} s^{-1} (Table 4). Ethanol (EtOH), which is a relatively inefficient positive charge scavenger, displayed another effect on the NpOH$^{\bullet+}$ when analyzed at $\lambda = 570$ nm. The overall absorption decreased on the addition of EtOH, and the 570 nm band only underwent slightly faster decay. The bimolecular rate constant determined from the linear variation of k_{obs} with the ethanol concentration was $k_{13b} = 6 \times 10^8$ dm^3 mol^{-1} s^{-1} (Table 4). As is typical for radical cations,[14] the transient band at 570 nm remained unaffected in O_2-saturated solutions. These findings also confirm the cationic nature of the transient band at 570 nm.

The NpOH$^{\bullet+}$ are formed in the charge transfer from solvent radical cations (reaction 8) and are subsequently scavenged in the presence of TEA (reaction 13a). Ethanol competes with the charge transfer (reaction 8) and, therefore, prevents the efficient formation of NpOH$^{\bullet+}$ (reaction 13c).

$$\text{2-NpOH}^{\bullet+} + \text{TEA} \rightarrow \text{TEA}^{\bullet+} + \text{2-NpOH} \qquad (13a)$$

$$\text{2-NpOH}^{\bullet+} + C_2H_5OH \rightarrow \text{2-NpO}^{\bullet} + C_2H_5OH_2^{\;+} \qquad (13b)$$

$$\text{BuCl}^{\bullet+} + C_2H_5OH \rightarrow {}^{\bullet}\text{BuCl} + C_2H_5OH_2^{\;+} \qquad (13c)$$

An analysis of the time profiles at 360, 470, and 570 nm (Figure 2b) shows that the 570 nm band of the solute radical cation (2-NpOH$^{\bullet+}$) is formed immediately. Only slightly delayed formation may be supposed at 360 and 470 nm (2-NpO$^{\bullet}$). In addition to the delayed formation of naphthoxyl radicals, a major portion was formed immediately after the pulse, which is explained by reaction 14.

$$\text{BuCl}^{\bullet+} + \text{2-NpOH} \rightarrow \text{2-NpO}^{\bullet} + \text{H}^{+}(\text{BuCl}) \qquad (14)$$

The delayed formation ought to proceed by the decay of solute radical cations by deprotonation (reaction 15), a process that is markedly slower and less efficient than in the case of phenols.[1]

$$\text{2-NpOH}^{\bullet+}, \text{BuCl} \rightarrow \text{2-NpO}^{\bullet} + \text{H}^{+}\ (\text{BuCl}) \qquad (15)$$

The absorption time profiles at 360 and 470 nm obtained in the presence of TEA revealed the absence of the delayed formation of naphthoxyl radicals. It is concluded that the solute radical cations are now converted to TEA$^{\bullet+}$ (reaction 13) instead of decaying by reaction 15. The TEA concentration-dependent depletion of 2-NpO$^{\bullet}$ seems to be caused by the competition of reactions 14 and 16.

$$\text{BuCl}^{\bullet+} + \text{TEA} \rightarrow \text{TEA}^{\bullet+} + \text{BuCl} \qquad (16)$$

Decay of Solute Radical Cations. When the fate of the solute radical cations
(2-NpOH$^{\bullet+}$) is analyzed, the competition of at least three reaction channels should be taken into account: (i) deprotonation (reaction 15), (ii) neutralization (reaction 17)

$$\text{2-NpOH}^{\bullet+} + \text{Cl}^{-} \rightarrow \text{products} \qquad (17)$$

and (iii) self-deprotonation by naphthol (reaction 18),

$$\text{2-NpOH}^{\bullet+} + \text{2-NpOH} \rightarrow (\text{2-NpOH}_2)^{+} + \text{2-NpO}^{\bullet} \qquad (18)$$

The initial part of the time profiles at 570 nm underwent slightly faster decay, without the additionally delayed formation of naphthoxyl radicals at increasing solute concentrations (5×10^{-4} to 1×10^{-1} mol dm^{-3}), which excludes reaction 18. The charge neutralization process, however, is affected by the dose rate. At the low dose rate of 20 Gy per pulse, the naphthol radical cation decayed by first-order kinetics with a lifetime of 3.7 μs. As the dose rate was increased to 50 Gy per pulse, its lifetime decreased to 1.5 μs. At much higher doses per pulse (about 200 Gy), the decay showed mixed kinetics, which (if at all) could be explained by a superposition of inhomogeneous effects with volume neutralization and reactions with hydrochloric acid produced by reaction 5b. These studies show that the decay of the naphthol radical cations is governed by neutralization and that other channels such as reactions 15 and 18 only play a minor role.

The decay of naphthoxyl radicals in BuCl could hardly be calculated exactly because of superpositions of radicals and radical cations. However, in aqueous solutions they were observed to decay by second-order kinetics with $2k = 4.5 \times 10^8$ dm^3 mol^{-1} s^{-1}, which should be corrected for BuCl by the viscosity-determined factor of 2 to give about 8×10^8 dm^3 mol^{-1} s^{-1}.

Effect of Solute Concentration. The 2-NpOH$^{\bullet+}$ yield (monitored at 570 nm) increased with solute concentration, reaching a saturation value at 10^{-2} mol dm^{-3} 2-NpOH. In contrast to this, the 2-NpO$^{\bullet}$ yield (determined at 350 and 475 nm) also showed an appreciable increase at higher solute concentrations (inset of Figure 2a). At naphthol concentrations higher than 2×10^{-2} mol dm^{-3}, a slight change in the spectral shape appears to be caused by increased absorption around 380−450 nm. At 5×10^{-2} mol dm^{-3} 2-NpOH the formation of a new band could clearly be seen. Figure 5 shows the transient optical absorption spectra obtained during pulse radiolysis of an N_2-saturated solution of 2-NpOH (5×10^{-2} mol dm^{-3}) in BuCl, 0.16 and 1.44 μs after the pulse. Although the absorption in the 350−370 nm region (which is due to naphthoxyl radicals) showed slight decay, increased absorption was observed in the 400−450 nm region during the same time, i.e., a new transient appeared.

Simultaneously with its delayed formation, the initial part of the 2-NpOH$^{\bullet+}$ time profile taken at 570 nm (inset of Figure 5) showed slightly faster decay ($k = 1.1 \times 10^6$ s^{-1}), which matched the formation of the new transient. Furthermore, it was found that adding a low concentration of TEA (1×10^{-3} mol dm^{-3})

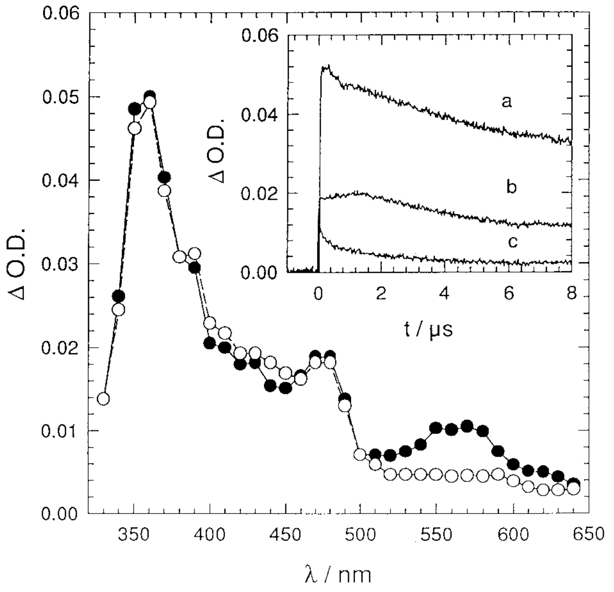

Figure 5. Transient optical absorption spectra obtained in pulse radiolysis of an N_2-saturated solution of 2-NpOH (5×10^{-2} mol dm^{-3}) in BuCl 0.16 (●) and 1.44 μs (○) after the pulse. The inset shows absorption time profiles obtained during pulse radiolysis of an N_2-saturated solution of 2-NpOH (5×10^{-2} mol dm^{-3}) in BuCl at 350 (a), 410 (b), and 570 nm (c).

quenched the formation of the new transient band around 400−450 nm. Thus, we concluded that this band observed only at high solute concentration is caused by a product of the ion molecule reaction of naphthol radical cations with naphthol (reaction 19) with a conceivable structure of a dimer stabilized by charge-transfer interaction as is known for condensed aromatics.[11,15]

$$2\text{-NpOH}^{\bullet+} + 2\text{-NpOH} \rightleftarrows (2\text{-NpOH})_2^{\bullet+} \qquad (19)$$

With $k_{19} = 3 \times 10^7$ dm^3 mol^{-1} s^{-1}, the dimerization rate is much smaller than those determined for pure aromatics. Such an ion−molecule reaction was not observed in the case of phenol and its sterically hindered derivatives.[1] However, for the naphthols it may be supposed that under favorable conditions of orbital overlap, dimer radical cations could be observed at high solute concentrations. Because of the planarity of the molecule, such an orbital overlap may be achieved in the case of naphthols.

Analogous pulse radiolysis studies performed with 1-NpOH in BuCl solution also revealed the formation of naphthoxyl radicals and solute radical cations. The kinetic and spectral parameters of the transient species formed from 1-NpOH are shown in Tables 1−5.

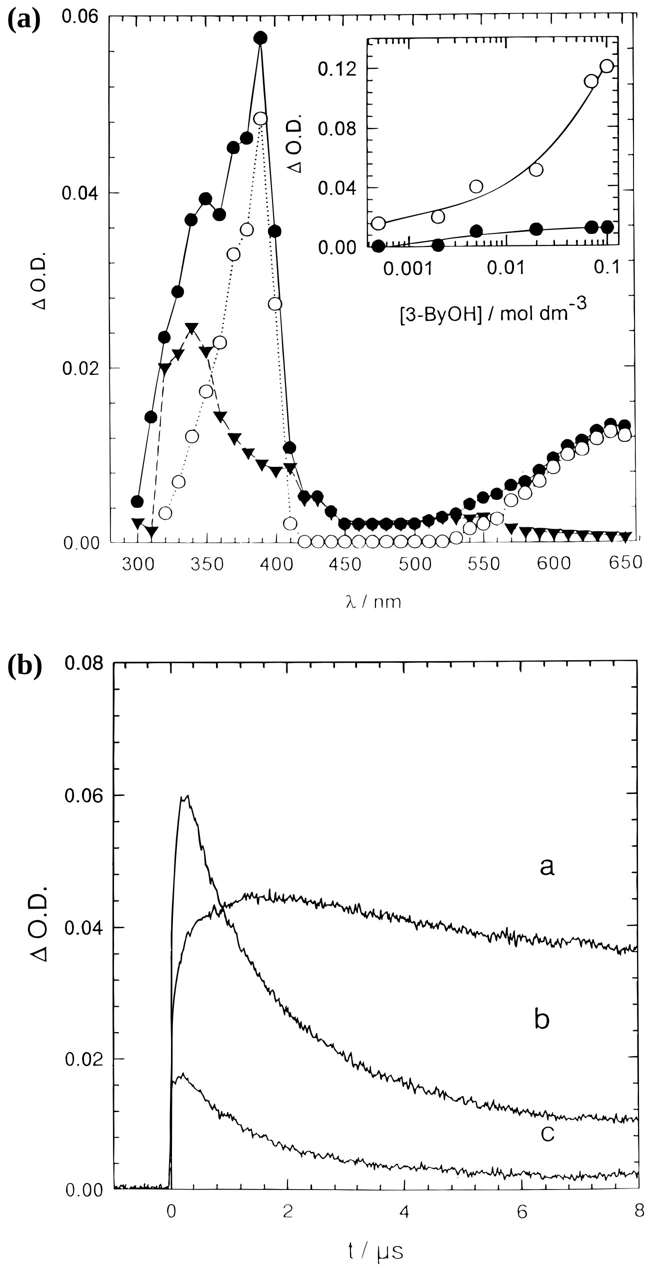

Figure 6. (a) Transient optical absorption spectra obtained in pulse radiolysis of an N_2-saturated solution of 3-ByOH (5×10^{-3} mol dm^{-3}) in BuCl in the absence (●) and in the presence of 1×10^{-3} mol dm^{-3} TEA (▼). The difference between the absorption spectra is shown as ○. The inset shows the variation of absorbance as a function of the solute concentration at 340 (○) and 650 nm (●). (b) Absorption time profiles obtained during pulse radiolysis of an N_2-saturated solution of 3-ByOH (5×10^{-3} mol dm^{-3}) in BuCl at 340 (a), 390 (b), and 650 nm (c).

3.2. Pulse Radiolysis of Hydroxybiphenyls. *Pulse Radiolysis of 3-ByOH.* Figure 6a shows the transient optical absorption spectrum obtained during pulse radiolysis of an N_2-saturated solution of 3-ByOH (5×10^{-3} mol dm^{-3}) in BuCl 300 ns after the pulse. It exhibits absorption bands with $\lambda_{\max} = 390$ and 650 nm with shoulders at 350, 370, 430 nm and a small broad absorption in the 450−550 nm region. Kinetic analysis of absorption time profiles indicates that the absorptions at 650 nm (curve c in Figure 6b) and at 390 nm (curve b, neglecting the slow background) showed similar kinetic behavior and decayed by first-order kinetics with $k = 5 \times 10^5$ s^{-1}. But the 340 nm absorption (curve a in Figure 6b) is long-lived and showed a partly delayed formation estimated to proceed with $k = 2.5 \times 10^6$ s^{-1}. This delayed formation was also observed in the 510−580 nm region. We state that in analogy to the findings of naphthol radiolysis, two kinds of transients are observed, 3-ByOH$^{\bullet+}$ and 3-ByO$^\bullet$. As expected for cations, in the presence of 1×10^{-3} mol dm^{-3} TEA, the transient absorptions at 650 and 390 nm were completly quenched (Figure 6a), whereas the broad and long-lasting absorption bands at $\lambda_{\max} = 340$ nm, shoulder at 430, and low broad absorption in the 450−550 nm region remained (Figure 6a), as is typical for aroxyl radicals. In the presence of TEA, the delayed formation of 3-ByO$^\bullet$ at 340 nm also disappeared. Thus, we can conclude that (i) 3-ByOH$^{\bullet+}$ is formed by the charge-transfer reaction with the solvent parent ions (reaction 20), (ii) in competition with this, fast 3-ByO$^\bullet$ formation takes place by deprotonation as shown

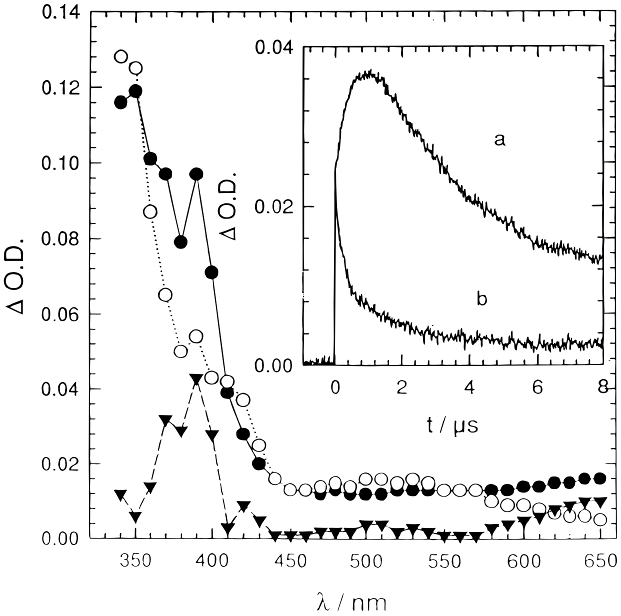

Figure 7. Optical absorption spectra obtained during pulse radiolysis of an N_2-saturated solution of 3-ByOH (0.1 mol dm^{-3}) in BuCl 0.16 (●) and 1.4 μs (○) after the pulse. The difference between these two spectra is shown as ▼. The inset shows absorption time profiles obtained during pulse radiolysis of 3-ByOH (0.1 mol dm^{-3}) in BuCl at 420 (a) and 650 nm (b).

in reaction 21, and (iii) a delayed deprotonation (reaction 22) of the solute cation 3-ByOH$^{\bullet+}$ was observed.

$$\text{BuCl}^{\bullet+} + \text{3-ByOH} \rightarrow \text{3-ByOH}^{\bullet+} + \text{BuCl} \qquad (20)$$

$$\text{BuCl}^{\bullet+} + \text{3-ByOH} \rightarrow \text{3-ByO}^{\bullet} + \text{H}^{+}(\text{BuCl}) \qquad (21)$$

$$\text{3-ByOH}^{\bullet+}, \text{BuCl} \rightarrow \text{3-ByO}^{\bullet} + \text{H}^{+}\ (\text{BuCl}) \qquad (22)$$

This situation closely resembles those observed in the naphthol system. Further evidence for the classification of absorption bands of 3-ByO$^{\bullet}$ radicals came from the similarity of the absorption spectrum obtained in BuCl to that spectrum obtained in the reaction of $N_3^{\bullet}$ radicals with 3-ByO^{-} (inset of Figure 3).

$$\text{3-ByO}^{-} + \text{N}_3^{\bullet} \rightarrow \text{3-ByO}^{\bullet} + \text{N}_3^{-} \qquad (23)$$

The yield of 3-ByOH$^{\bullet+}$ increased with solute concentration, reaching saturation at 5×10^{-3} mol dm^{-3} (inset of Figure 6a). However, for 3-ByO$^{\bullet}$ a considerable yield increase was also observed at higher solute concentrations. The rate constant of the delayed formation (reaction 22) of 3-ByO$^{\bullet}$ radicals remained independent of solute concentration. However, for solute concentrations greater than 7×10^{-2} mol dm^{-3}, another absorption band ($\lambda_{max} = 420$ nm) appeared. Figure 7 shows this situation using transient spectra taken of a 0.1 M solution of 3-ByOH in BuCl. The delayed formation at 340 and 520 nm of 3-ByO$^{\bullet}$ radicals is independent of the solute concentration and appears at the same rate as at low concentrations. However, the 3-ByOH$^{\bullet+}$ decay profiles at 380 and 650 nm were accelerated in a pseudo-first-order manner, and simultaneously, the increasing absorption at 410−430 nm was observed. Corresponding to the 1-NpOH experiments described in the former chapter, we attribute this delayed transient formation (inset of Figure 7) to the ion molecule reaction 24 resulting in a product of a conceivable dimer radical cation structure. The rate constant of the forward reaction was determined to be $k_{24} = 4.5 \times 10^{7}$ dm^3 mol^{-1} s^{-1}.

$$\text{3-ByOH}^{\bullet+} + \text{3-ByOH} \rightleftarrows (\text{3-ByOH})_2^{\bullet+} \qquad (24)$$

Analogous pulse radiolysis studies with 2-ByOH and 4-ByOH in BuCl were carried out also. The kinetic and spectral parameters for various transient species formed from these compounds are presented in Tables 1−5.

3.3. Effect of Solute Structure. *Kinetic Considerations.* The charge transfer from radiolytically generated parent ions to added solutes (e.g., reaction 25) is a satisfactory way of producing radical cations of substances with an ionization potential lower than the nonpolar solvent used.[15,16]

$$\text{BuCl}^{\bullet+} + \text{S} \rightarrow \text{S}^{\bullet+} + \text{BuCl} \qquad (25)$$

In the case of scavenger (S) concentrations less than 2×10^{-3} mol dm^{-3}, a free-ion reaction is concerned, comparable with those of the usual one-electron oxidants such as $N_3^{\bullet}$, $SO_4^{\bullet-}$, etc. in polar systems but exhibiting the advantage of the relative stability of the product radical cation. Hence, alkanes, cycloalkanes, and also alkyl chlorides are used for pulse radiolytic studies of charge-transfer phenomena. When the rate constants of solute cation formation are determined by analyzing the influence of the scavenger on the time profiles of the parent cations, the rate constants k_{25} are sometimes a little higher than the diffusion-controlled limit (cf. Table 1). The reason for this effect probably consists of the initially incomplete relaxation of the solvent cations due to their "positive hole" character[14] and phasing-out of their inhomogeneous distribution.[17] But the solute cations $S^{\bullet+}$ are in a completely free and relaxed state.

As already reported in a previous paper,[1] in the case of phenols (mainly sterically hindered), charge-transfer reaction 25 generates, within our time resolutions of about 10 ns, two products in an apparently competing manner: phenol radical cations and phenoxyl radicals, with the latter dominating by far. This is described by reactions 1a and 1b). Furthermore, it should be mentioned that the rapid formation of phenoxyls (reaction 1b) does not proceed by the deprotonation of phenol radical cations, which has been found to be a delayed process.[1]

The charge-transfer studies presented here with naphthols and hydroxybiphenyls of different OH substitution patterns seem to provide a deeper insight into the mechanism described above. Figure 8 gives a general reaction scheme of the cation reactions studied. In the reaction with parent cations for the naphthols and hydroxybiphenyls, in all cases a much higher portion of radical cations ArOH$^{\bullet+}$ was observed (cf. Table 5) than for phenols. Furthermore, the lifetime of these species also lasts much longer, being determined mainly by neutralization (reactions 2a and 17) of the charge. At this point let us include in the discussion the larger size of the aromatic system in comparison to the OH substituent. Hence, to explain the competition of the parallel cation (1a, 8, 20) and oxyl radical (1b, 14, 21) formation, we propose a mechanism that takes into account the geometry of the collision of the reacting species BuCl$^{\bullet+}$ and ArOH, either at the aromatic part or at the polar hydroxyl group of the solute molecule. In the first case the formation of an aromatic-dominated radical cation ought to occur with charge delocalization throughout the whole molecule. In the collision near the OH substituent just before charge delocalization, an immediate deprotonation of the solute radical cation in a complexed state should take place. This is indicated in the reaction scheme as the charge-transfer situation given in brackets. Hence, reaction channel 1b immediately yields ArO$^{\bullet}$ and protons that are stabilized afterward by solvatization by the surroundings, in this case BuCl.

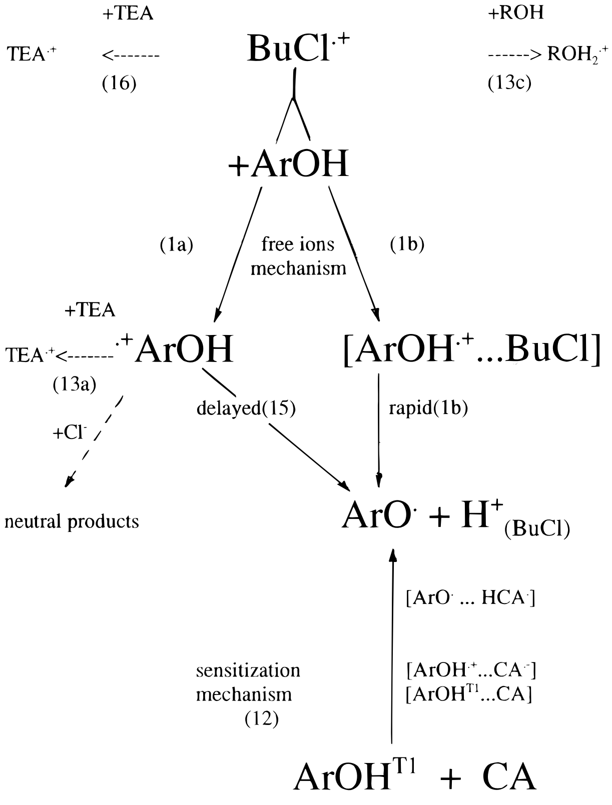

Ar = phenyl, naphthyl, biphenylic ring with different substitution patterns
CA = chloranil **TEA** = triethylamine **ROH** = alkanol

Figure 8. Reaction scheme depicting the charge-transfer processes involving different kinds of phenolic compounds such as one-ring phenols, naphthols, and hydroxybiphenyls.

TABLE 5: Lifetime and Absorbance of the Solute Radical Cations of Different Solutes ArOH Formed in BuCl[a]

solute cation $ArOH^{\bullet+}$	λ_{max} (nm)	lifetime (μs)	$G\epsilon \times 10^{-3}$
phenol	~420	<0.2	
2,6-di-*tert*-butylphenol	440	0.3	
4-methoxy phenol	400	0.5	3.5
2,6-di-*tert*-butyl-4-methoxyphenol	460	0.7	1.1
1-NpOH	600	1.9	0.9
2-NpOH	570	1.5	1.0
2-ByOH	600	2.4	1.5
3-ByOH	650	2.1	2.6
4-ByOH	650	2.1	2.8

[a] Concentration of the solute = 5×10^{-3} mol dm^{-3}. Dose = 52 Gy per pulse.

This effect of competition between charge transfer 1a and deprotonation 1b was only observed in the case of the reaction of free ions with the phenolic scavenger. In the triplet-sensitized electron transfer 12 checked for the donor–acceptor pair 2-NpOH^{T1} and chloranil, only naphthol radicals are formed, i.e., an immediate deprotonation of the $NpOH^{\bullet+}$ occurred within the ion pair. This can clearly be seen when comparing transient spectra of triplet-sensitized reaction 12 given in Figure 4 with those obtained in the ion–molecule reactions 1a and 1b involving the free ions of the solvent given in Figure 5.

The time-resolved deprotonation of the stabilized and delocalized radical cation $^{\bullet+}ArOH$ (left side of the scheme) proceeds in a delayed manner (reaction 15). Clear kinetic connections were also found for this reaction channel by observing the decay of $ArOH^{\bullet+}$ and the formation of one part of $ArO^{\bullet}$.

The other reactions contained in the reaction scheme (Figure 8) illustrate the reactivity of the solute radical cations against added further scavengers (TEA, alcohol), which are commonly used for radical cation identification. As experimentally demonstrated in this paper, TEA acts in low concentration as a charge scavenger for the $ArOH^{\bullet+}$, whereas at $>10^{-3}$ mol dm^{-3} mainly the solvent parent cations are quenched. Ethanol rapidly quenches the solvent parent ions by its deprotonation; the deprotonation of $ArOH^{\bullet+}$ seems to be slower and could not be well characterized.

Charge Distribution and Geometry of the Transition State. The lifetime of the radical cation formed under identical conditions of dose and solute concentration was compared for different phenols, naphthols, and hydroxybiphenyls (Table 5). In the case of phenols, it was observed to increase in the presence of the electron-releasing methoxy group, and alkyl substituents seem to have a similar, albeit minor, effect. Hence, lifetimes for phenol radical cations were in the range 0.5–0.7 μs. In the case of naphthols and hydroxybiphenyls, lifetimes were in the ranges 1–2 and 2–3 μs, respectively. As already postulated, the lifetime dependence on the molecular structure could be due to the influence of the aromatic moiety. This also seems to be supported by the remarkable difference in the relative yields ($G\epsilon$) of the radical cations (cf. Table 5).

To learn more about the influence of the electronic structure of the transient species, we undertook semiempirical open-shell quantum chemical calculations. By use of PM3[18,19] wave functions, the geometries and energies for the ground and the excited states of phenols, naphthols, and hydroxybiphenyls were calculated using HyperChem 5.01. The geometry optimization of all compounds was performed in a vacuum with the Polac–Ribiere conjugate gradient method in the unrestricted Hartree–Fock (UHF) approximation. The direct inversion in the iterative subspace (DIIS) method was used for better convergence of self-consistent field (SCF) calculations of the electronic structure. HyperChem uses atomic charges, which are commonly used in molecular orbital theory. The calculated quantities are only approximately related to experiment, but they provide a reasonable representation of the 3D charge distribution within a molecule.

As expected, in each case part of the positive charge is nearly uniformly distributed among all H atoms of the aromatic rings. The oxygen polarizes the molecule in such a way that the phenolic proton and the neighboring C atom have the highest charges. In the case of the unsubstituted phenol, the carbon in the para position to the OH group represents an additional positive charge localization center. In the case of the naphthol as well as hydroxybiphenyl isomers, the second aromatic moiety contributes to a further charge localization. There are no real systematics for a marked charge localization difference in the carbon atoms except that being substituted by OH. But the charge delocalization in the H atoms shows more or less uniform behavior, expressed in very similar positive values. Charge delocalization thus takes place throughout the whole aromatic molecule. Exceptions from this observation include 2-naphthol and 3-hydroxybiphenyl, where in the carbon skeleton an additional charge localization center has been found in the 4- and 1-position, respectively. The typical charge distribution of a phenolic radical cation is shown in Chart 1 using the example of 2-naphthol and 3-hydroxybiphenyl.

With respect to the geometry of the transition state of the studied charge transfer reactions 1a and 1b, we analyzed possible stable configurations for the electron jump using the same approach. Generally speaking, there exists in each case a rapid

CHART 1: 2-Naphthol (Left) and 3 Hydroxybiphenyl (Right)

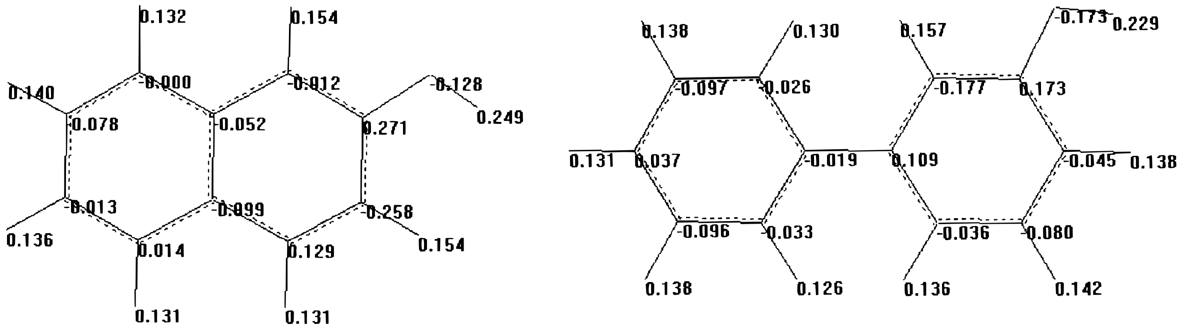

and geometry-unspecific charge transfer to the aromatic moiety, as is also known to proceed over relatively long distances.[20] However, the calculations also yielded a stable geometry for the charge transfer from the $BuCl^{\bullet+}$ to the phenolic group, which shows a clear distance between the Cl atom of the BuCl and the phenolic proton of 1.8 Å. This gives rise to the postulated mechanism involving synchroneous electron transfer and a deprotonation of the phenolic group. In view of the proton affinity of a halocarbon such as BuCl, there is a considerable proton affinity (PA) of about 150 kcal mol^{-1}, i.e., quite comparable with those of a corresponding alcohol (e.g., $PA_{CH3Cl} = 163$ kcal mol^{-1}, $PA_{CH3OH} = 181$ kcal mol^{-1}).[21] Hence, in the case of BuCl the stable electron-transfer geometry at the phenolic group ought to favor electron transfer with immediate deprotonation resulting in phenoxyl radicals and solvent-stabilized protons. This interpretation supports the mechanism established experimentally.

4. Conclusions

Owing to their low ionization potential, the phenols are good electron donors and can react with the solvent radical cations ($BuCl^{\bullet+}$) in two ways, charge transfer 1a and immediate deprotonation 1b. The yield of radical cations of phenols (C_6H_5-OH) is low,[1] and reaction 1b seems to dominate. In the case of naphthols and hydroxybiphenyls, the solvent radical cations react in comparable parts via charge transfer 1a and deprotonation 1b. By contrast, in the triplet-sensitized electron transfer (reaction 12) examined only for the pair naphthol triplet and choranil, only naphthoxyl radicals seemed to be formed, which is explained by electron transfer with subsequent proton transfer within the ion pair.

As also supported by quantum chemical calculations, for naphthols and hydroxybiphenyls the positive charge is stabilized because of the extended aromatic moiety, which is also experimentally demonstrated by comparison of the lifetimes of the radical cations $ArOH^{\bullet+}$. Owing to the increased stability of the radical cations of naphthols and hydroxybiphenyls, they decay to a considerable extent via the charge neutralization process, whereas the radical cations of phenols decay exclusively via the deprotonation mechanism.[1]

References and Notes

(1) Brede, O.; Orthner, H.; Zubarev, V. E.; Hermann, R. *J. Phys. Chem.* **1996**, *100*, 7097.

(2) Schnabel, W. *Polymer Degradation*; Hanser: Munich, 1992.

(3) Scott, G. *Atmospheric Oxidation and Antioxidants*; Elsvier: Amsterdam, 1993; Vols. I, II.

(4) (a) Becconsall, J. K.; Clough, S.; Scott, G. *Proc. Chem. Soc*. **1959**, 308. (b) Bennett, J. E. *Nature* **1960**, *186*, 385.

(5) (a) Brede, O.; Hermann, R.; Mehnert, R. *Radiat. Phys. Chem.* **1986**, *28*, 507. (b) Brede, O. *Radiat. Phys. Chem.* **1987**, *29*, 369. (c) Brede, O.; Hermann, R.; Mehnert, R. *J. Chem. Soc., Faraday Trans. 1* **1987**, *83*, 2365.

(6) (a) Land, E. J.; Porter, G.; Strachan, E. *Trans. Faraday Soc.* **1961**, *57*, 1885. (b) Land, E. J.; Porter, G. *Trans. Faraday Soc.* **1963**, *59*, 2016. (c) Land, E. J.; Ebert, M. *Trans. Faraday Soc.* **1967**, *63*, 1181. (d) Bansal, K. M.; Fessenden, R. W. *Radiat. Res*. **1976**, *67*, 1.

(7) (a) Dixon, W. T.; Murphy, D. *J. Chem. Soc., Faraday Trans. 2* **1976**, *72*, 1221. (b) Dixon, W. T.; Kok, P. M.; Murphy, D. *J. Chem. Soc., Faraday Trans. 2* **1977**, *73*, 709. (c) Dixon, W. T.; Murphy, D. *J. Chem. Soc*., *Faraday Trans. 2* **1978**, *74*, 432.

(8) Holtman, D. M.; Murphy, D. *J. Chem. Soc., Faraday Trans. 2* **1979**, *75*, 1637.

(9) Kesper, K.; Diehl, F.; Simon, J. G. G.; Specht, H.; Schweig, A. *Chem. Phys.* **1991**, *153*, 511.

(10) Zubarev, V. E.; Brede, O. *Acta Chem. Scand.* **1997**, *51*, 224.

(11) (a) Robinson, A. J.; Rodgers, M. A. J. *J. Chem. Soc., Faraday Trans. 1* **1973**, *69*, 2036. (b) Mehnert, R.; Brede, O.; Naumann, W. *Ber. Bunsen-Ges. Phys. Chem.* **1982**, *86*, 525.

(12) Alfassi, Z. B.; Schuler, R. H. *J. Phys. Chem.* **1985**, *89*, 3359.

(13) (a) Carmichael, J.; Hug, G. *J. Phys. Chem. Ref. Data* **1986**, *15*, 135. (b) Brede, O.; Mehnert, R.; Naumann, W.; Teply, J. *Ber. Bunsen-Ges. Phys. Chem.* **1985**, *89*, 1036. (c) Gschwind, R.; Haselbach, E. *Helv. Chim. Acta* **1979**, *79*, 941.

(14) Brede, O.; Bös, J.; Helmstreit, W.; Mehnert, R. *Radiat. Phys. Chem.* **1982**, *19*, 1.

(15) Busi, F. In *The Study of Fast Processes and Transient Species by Electron Pulse Radiolysis*; Baxendale, J., Busi, F., Eds.; D. Reidel: Dordrecht, 1982; p 417.

(16) Brede, O.; Mehnert, R.; Naumann, W. *Chem. Phys.* **1987**, *115*, 279.

(17) Warman, J. M. In *The Study of Fast Processes and Transient Species by Electron Pulse Radiolysis*; Baxendale, J., Busi, F., Eds.; D. Reidel: Dordrecht, 1982; p 433.

(18) Collins, J. B.; Schleyer, P. V.; Binkley, J. S.; Pople, J. A. *J. Chem. Phys.* **1976**, *64*, 5142.

(19) Stewart, R. F. *J. Chem. Phys.* **1970**, *52*, 438.

(20) Pilling, M. J.; Rice, S. A. *J. Chem. Soc., Faraday Trans. 2* **1975**, *71*, 1563.

(21) Tabata, Y., Ito, Y., Tagawa, Eds. In *Handbook of Radiation Chemistry*; CRC Press: Boca Raton, FL, 1991; p 204.